

Seawater-Based Triboelectric Nanogenerators for Marine Anticorrosion

Chuguo Zhang, Baofeng Zhang, Wei Yuan, Ou Yang, Yuebo Liu, Lixia He, Zhihao Zhao, Linglin Zhou, Jie Wang,* and Zhong Lin Wang



Cite This: <https://doi.org/10.1021/acsami.1c23575>



Read Online

ACCESS |



Metrics & More



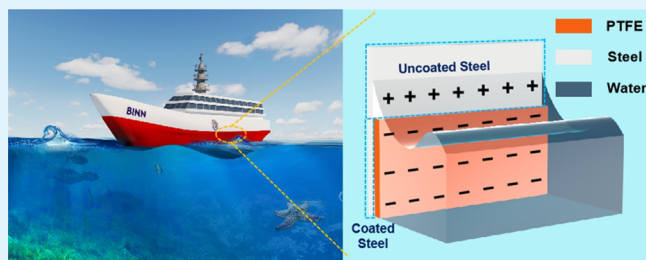
Article Recommendations



Supporting Information

ABSTRACT: The liquid–solid triboelectric nanogenerator is broadly studied for its self-powered sensing and blue energy harvesting, thanks to its low wear and highly efficient contact. However, the corresponding research studies focusing on deionized-water liquid–solid triboelectric nanogenerators (DL-TENGs) and seawater-type liquid–solid TENGs (SL-TENGs) are rarely being carried out at present. Here, a SL-TENG is fabricated by applying a dielectric film as the organic coating and coated and uncoated steel hull as the two electrodes. Based on the reasonable material selection of the dielectric film, the SL-TENG showed excellent performance, which benefits from the good triboelectrification performance and weak ion adsorption effect. In addition, compared with commercial marine anticorrosive coatings, the friction coefficient of the SL-TENG with the seawater can be reduced 43.8%, which is significantly beneficial to reduce the sailing resistance of ships. More importantly, the uncoated steel electrode can obtain a high potential in highly corrosive seawater, which can enable it to perform the function of marine anticorrosive agents. Our finding provides a potential strategy to evade the marine anticorrosion of ships.

KEYWORDS: seawater, blue energy, liquid–solid, marine anticorrosion, triboelectric nanogenerator



1. INTRODUCTION

With the deepening of economic globalization, ocean, which takes up 70% of the earth's surface, is closely related to human production and life in blue energy harvesting, marine engineering construction, maritime transport, and so forth.^{1–3} However, the harsh marine environment with the characteristics of high salinity and highly corrosive nature also has a very adverse effect on human marine activities. Especially, high corrosiveness will seriously damage all kinds of marine equipment. Consequently, various marine anticorrosion technologies have been developed to extend the service life of marine equipment, such as marine anticorrosive coatings and electrochemical protection technology with impressed current.^{4–6} However, some toxic substances used in marine anticorrosive coatings affect the marine ecological environment and the lack of marine electric power cannot provide necessary guarantee for the electrochemical protection technology with the impressed current, which significantly restricts the application of both the abovementioned technologies.^{7,8}

As a new energy collection technology, triboelectric nanogenerators (TENGs) have been widely used in many fields, such as in self-powered sensing, high-voltage sources, and micro-/nanoenergy since they were invented in 2012.^{9–12} Besides, thanks to their advantages of light weight, low cost, and high efficiency at low frequency, TENGs are considered as an effective water wave energy collection technology.^{13,14} As

they avoid the serious wearing issue of solid–solid triboelectric nanogenerators (SS-TENGs), liquid–solid triboelectric nanogenerators, which are based on the coupling of triboelectrification and the electrostatic induction effect between liquid and solid triboelectric materials, have been extensively researched to harvest raindrop energy and water waves.^{15–22} However, the related research studies mainly focused on deionized-water liquid–solid triboelectric nanogenerators (DL-TENGs) and seawater-type liquid–solid triboelectric nanogenerator (SL-TENGs) are seldom carried out.^{23–27} In addition, all kinds of SS-TENGs and DL-TENGs have been designed to improve the marine anticorrosion capability of the corresponding device by collecting water wave energy and using electrochemical protection methods with the impressed current.^{28–31} However, due to the application of rectifiers, seawater-resistant carbon electrodes, and additional power supply, the system composition in this method is significantly complex. Therefore, it is very important to develop a new

Received: December 6, 2021

Accepted: January 19, 2022

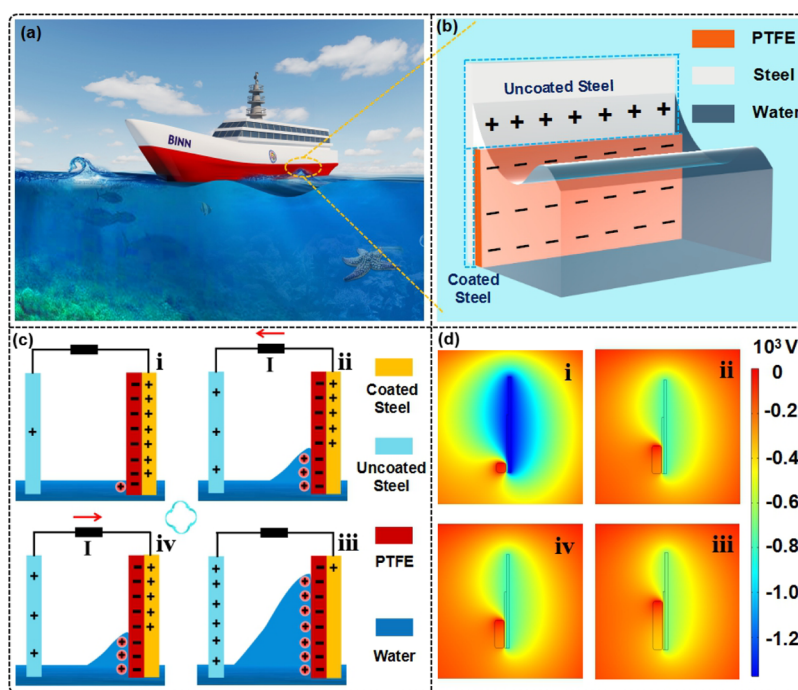


Figure 1. Structural design and working mechanism of the SL-TENG. (a) Device configuration of the SL-TENG installed on the hull. (b) Schematic representation structure for the SL-TENG. (c) Electricity generation principle of the SL-TENG. (d) Voltage potential distribution of the SL-TENG at different states by COMSOL simulation.

marine anticorrosion technology with a simple composition which is based on the triboelectric technique.

In this work, we report a SL-TENG which consists of a dielectric film as the organic coating and coated and uncoated steel hull as the two electrodes. According to the material optimization of the dielectric film, the SL-TENG shows good output performance because the used dielectric film exhibits good triboelectrification performance and weak ion adsorption effect in seawater. Besides, the dielectric materials of the SL-TENG can reduce the friction coefficient of the SL-TENG in seawater to about half compared with the commercial marine anticorrosive coatings. This result is conducive to reduce the sailing resistance of ships. More importantly, the uncoated steel electrode in seawater shows marine anticorrosion properties; this is because the SL-TENG can endow the relative steel with a higher potential. In a word, our finding provides a novel method toward self-powered marine anticorrosion.

2. RESULTS AND DISCUSSION

2.1. Structural Design and Working Mechanism. As one of the crucial transportation methods, shipping with the advantages of huge carrying capacity, low transportation costs, and low requirements for transporting goods is significantly popular in the global freight market. These advantages come from the world's vast merchant fleet, but reducing complex maintenance costs in a highly corrosive marine environment is the main challenge for the further development of shipping. The current anticorrosion coating of vessels is mainly based on the principle that the anticorrosion insulation layer can isolate the hull from the ocean environment. However, the anticorrosive insulating layer can easily suffer from mechanical damage due to its thin characteristics and is especially prone to cracking in the process of application. Therefore, the damage of the insulation layer will cause the steel hull to suffer from serious corrosion, endangering the safety of the ship.

Therefore, a new technology with marine anticorrosion functions is urgently needed for reducing the maintenance costs of shipping. Here, inspired by the liquid–solid triboelectric nanogenerator with the characteristics of low wear and high efficient contact, a SL-TENG is designed to improve the marine anticorrosion ability, which can be fabricated on the hull (Figure 1a). The detailed structure of the SL-TENG is displayed in Figure 1b, which is composed of a coated steel electrode, an external polytetrafluoroethylene (PTFE) layer, and an uncoated steel electrode. When the ocean wave near the hull drives the seawater to slide up and down on the PTFE surface, a corresponding electron transfer occurs between the coated steel electrode and the uncoated steel electrode. Meanwhile, due to good triboelectric performance and weak ion adsorption effect, the PTFE surface is negatively charged, while the coated and uncoated steel electrodes are positively charged.^{28,32} Therefore, since the uncoated steel electrode is positively charged, its ability to lose electrons is greatly reduced and thus it can remain anticorrosive even in highly corrosive marine environments. Notably, the surface of PTFE dielectric materials with a good micro-/nanostructure is beneficial to improve the output performance of the SL-TENG and the hydrophobicity of the PTFE surface (Figure S1). Figure 1c shows the operative principle of the SL-TENG with a complete cycle. As a kind of excellent triboelectric material, the PTFE surface will generate negative charges due to the triboelectric effect when the water moves back and forth on the PTFE surface. At the same time, the corresponding positive charges will transfer into the coated and uncoated steel electrode to meet the electrostatic equilibrium (Figure 1ci). Since water gradually rises on the PTFE surface, the negative charge on the PTFE surface will be partially screened by the resulting electrical double layer (Figure S2), which will make the electrons on the uncoated steel electrode flow into the coated steel electrode to balance the different potentials distributed on

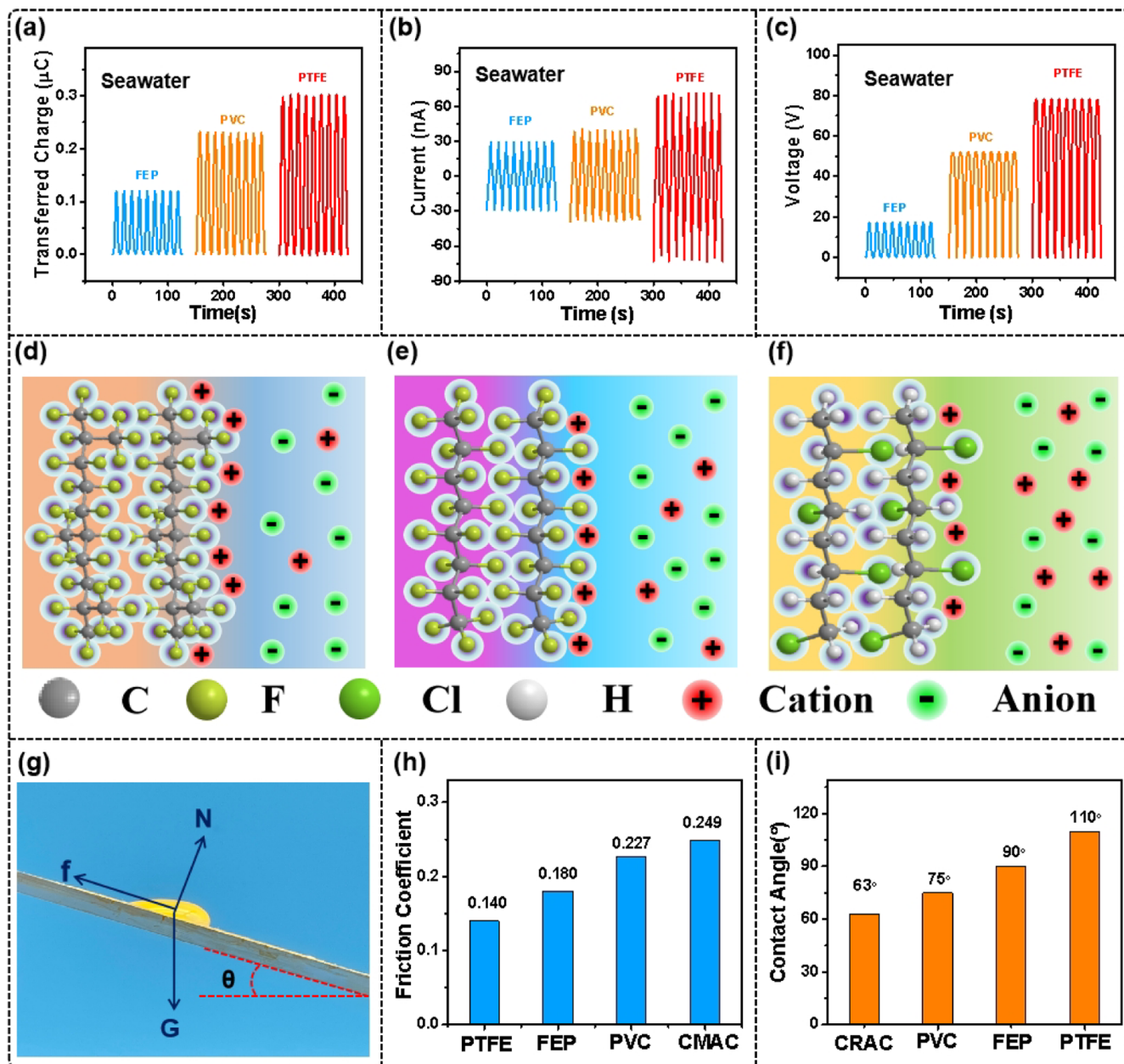


Figure 2. Characterization of the performances of the SL-TENG: (a) transferred charges, (b) short-circuit current, and (c) open-circuit voltage of the SL-TENG with different dielectric materials. Schematic diagram of ion adsorption on the FEP material surface (d), PTFE material surface, and (e) PVC material surface. (g) Force analysis diagram of a water droplet on an inclined material surface. (h) Friction coefficient of a water droplet on different materials. (i) Contact angles of different materials with seawater.

the two electrodes (Figure 1bii). When water reaches the highest position on the PTFE surface, the maximum transferred charges between the uncoated steel electrode and the coated steel electrode will be achieved (Figure 1ciii). Subsequently, with the water on the PTFE surface gradually falling back, a current from the uncoated steel electrode to the coated steel electrode is generated to compensate for the electrostatic potential difference between the two electrodes (Figure 1civ). Therefore, as the water on the PTFE surface rises and falls, it creates a constant alternating current between the uncoated and coated steel electrodes. Meanwhile, in order to better clarify the operation principle of the SL-TENG, the ideal potential distribution of the SL-TENG at different positions is simulated by using finite-element analysis (COMSOL Multiphysics) (Figure 1d). When water recip-

rocates on the surface of PTFE, a different potential distribution occurs on the uncoated and coated steel electrode, which is a good demonstration of the operation principle of the SL-TENG. In addition, the potential of the uncoated steel electrode rises during the working process of the SL-TENG and it has the relevant marine anticorrosion properties.

2.2. Output Performances of the SL-TENG. As seawater accounts for 97% of the world's water resources, which provides a vast space for the application of SL-TENGs, we design a SL-TENG by using natural seawater (Figure S3) and then the relative output performance of the SL-TENG with different dielectric materials is researched. The output performance of the SL-TENG with different dielectric materials is depicted in Figure 2a–c, and the transferred charges, short-circuit current, and open-circuit voltage of the

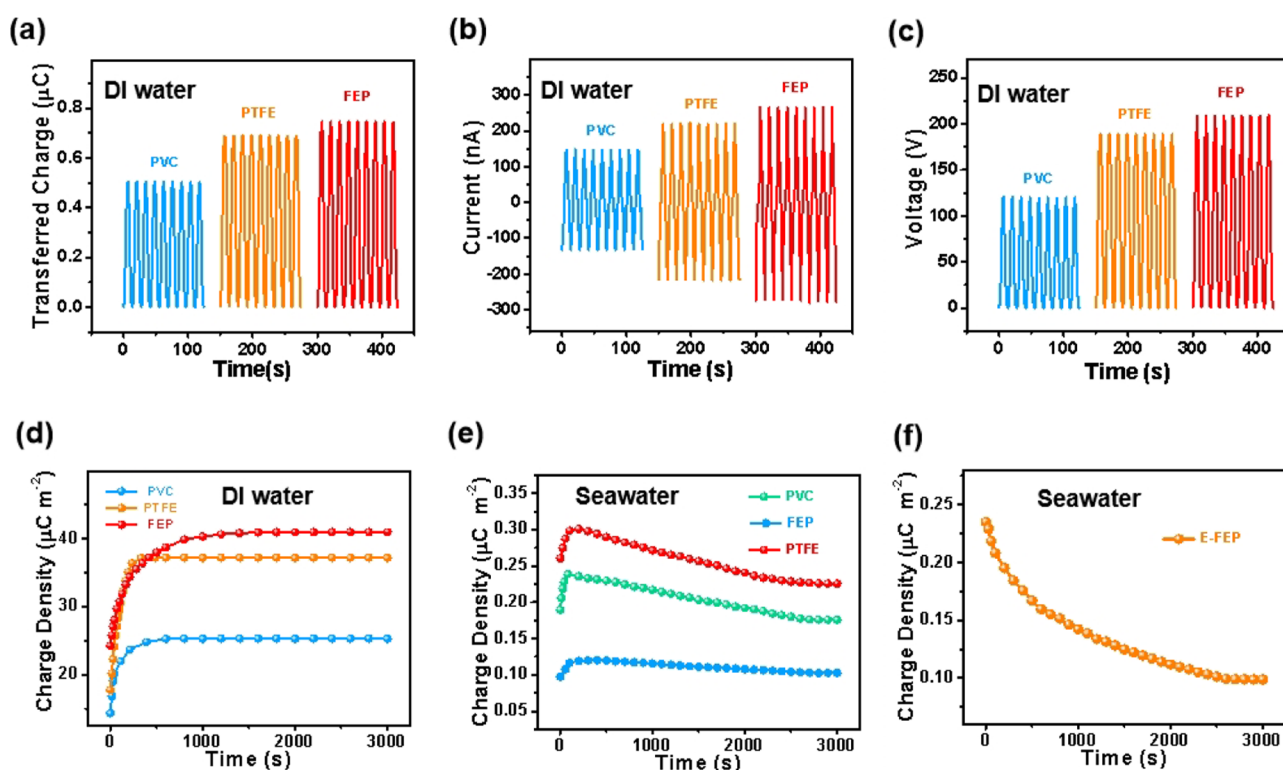


Figure 3. Characterization of performances of the DL-TENG. (a) Transferred charges, (b) short-circuit current, and (c) open-circuit voltage of the DL-TENG with different dielectric materials. (d) Charge density changing curve of the DL-TENG with different dielectric materials. (e) Charge density changing curve of the SL-TENG with different dielectric materials. (f) Charge density changing curve of the SL-TENG with the electret dielectric materials.

SL-TENGs with the fabrication of poly(vinyl chloride) PVC, PTFE, and fluorinated ethylene propylene (FEP) are 0.12, 0.23, and 0.30 μC ; 30, 40, and 70 nA; 17, 52, and 78 V, respectively. It is obvious that the SL-TENG with PTFE shows the best output performance and the possible reason is that the excess fluorinated methyl groups on the surface of the FEP dielectric material and the complex stereostructure of fluorinated methyl groups will make it absorb more cations and then greatly weaken the output performance of the SL-TENG fabricated by it compared with PTFE and PVC (Figure 2d–f). More detailed mechanisms are needed to be further researched in future work. In addition, for the application of the SL-TENG in the hull, the friction coefficient of seawater with a dielectric material surface will be crucial for reducing the seawater resistance of sailing ships. An inclined surface is designed to measure the corresponding friction coefficient by measuring the inclined angle required for a seawater droplet composed of seawater to roll on the inclined surface with different materials, and the related measuring principle is displayed in Figure 2d and Note S1. In addition, in order to more objectively verify the effect of the SL-TENG on seawater resistance of ships, a commercial marine anticorrosive coating (CMAC) for ships is studied as a reference, and the component of the CMAC is chlorinated rubber. Figure S4 shows the inclination angle of a water droplet beginning to slide on different materials. It can be found that PTFE achieves the minimum inclined angle. The friction coefficient and frictional force of a seawater droplet on different materials are shown in Figures 2e and S5, and it is obvious that PTFE has a minimum friction coefficient, which is significantly beneficial to reduce the seawater resistance of sailing ships. Compared with

the CMAC under the same conditions, PTFE can reduce the sailing resistance of ships by 43.8%. The reason behind this is that the seawater on the PTFE surface with an excellent surface microstructure has a minimum contact angle (Figures 2f, S6, and S7), which can help the seawater droplet to generate a greater rolling torque and reduce the related contact area as it rolls across the surfaces (Figures S8 and S9). Therefore, the advantages of using PTFE for the fabrication of the SL-TENG are significantly beneficial to reduce the sailing resistance of ships.

2.3. Output Performance Comparison of the DL-TENG and SL-TENG. As is known to all, there are a lot of anions and impurities in seawater, which often adversely affect the output performance of liquid–solid TENGs.^{32,33} In order to provide guidance for improving the output performance of SL-TENGs, which refers to the structure of the SL-TENG shown in Figure S3, a DL-TENG with the same structure as the SL-TENG is fabricated by using deionized water to replace natural seawater and then research the relative output performance (Figure S10). As depicted in Figure 3a–c, the transferred charges, short-circuit current, and open-circuit voltage of the DL-TENGs fabricated by PVC, PTFE, and FEP are 0.504, 0.684, and 0.742 μC ; 145, 220, and 268 nA; 120, 188, and 210 V, respectively. It is easy to find that the output performance of the DL-TENG is obviously higher than that of the SL-TENG. The relevant reason is that there is no large amount of anions and cations in deionized water (Note S2). As shown in Figure S11, due to the high electronegativity of the dielectric material surface, when it is immersed in seawater containing a large number of cations and anions, its surface will gradually absorb the corresponding cation to balance the

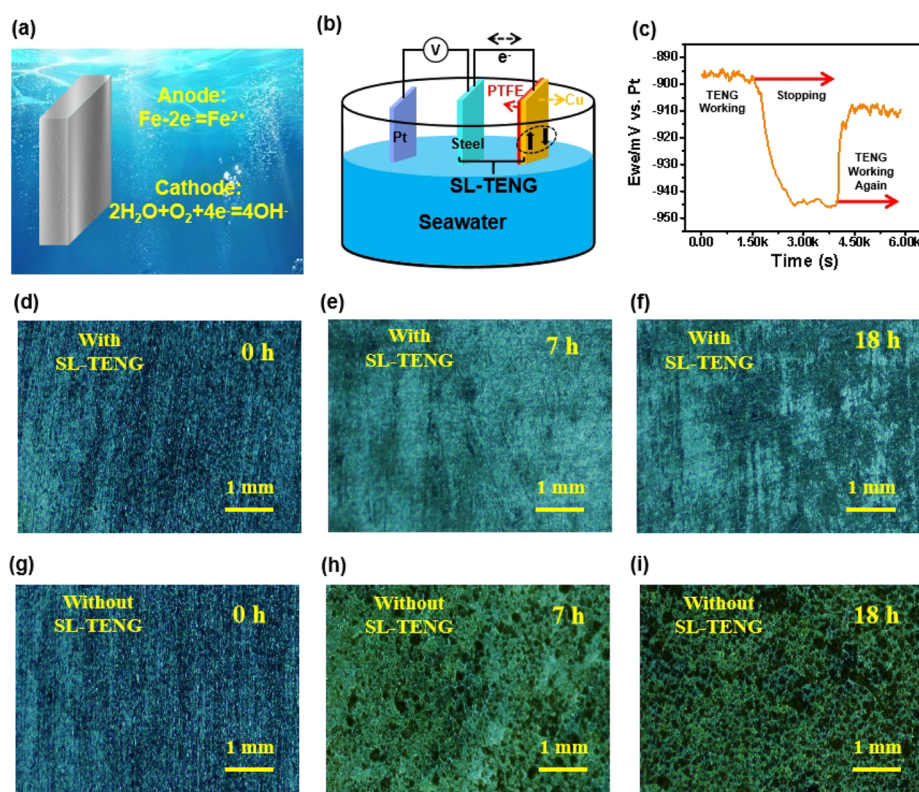


Figure 4. Measurement of the SL-TENG with marine anticorrosion function. (a) Mechanism of the most common marine corrosion of steel in seawater. (b) Schematic diagram of the potentiometric monitoring of steel electrodes immersed in seawater. (c) Potential change of the steel electrode relative to the Pt electrode when the SL-TENG is immersed in seawater in different states. Light microscopy image of the steel electrode surface with the SL-TENG (d–f) and without the SL-TENG (g–i) at different times.

negative charges so that the surface charge density of the dielectric material will gradually decrease. In addition, the same DL-TENG and SL-TENG are fabricated by using the nylon film, which is usually positively charged, as the dielectric material. It is not difficult to find that the corresponding output performance of the DL-TENG and SL-TENG is sharply reduced compared with the other three kinds of dielectric materials (Figure S12). The reason behind this is that water and nylon are both positive materials in the triboelectric sequence table, and their triboelectric performance is poor. Therefore, the selection of an electronegative dielectric material is more benefiting to obtain a SL-TENG with higher output performance. Meanwhile, since FEP has the best triboelectric performance and no strong influence of ion adsorption in the DL-TENG, the DL-TENG fabricated by FEP shows the best output performance, which is the same as the SS-TENGs (Figures S13–S16 and Note S3). In addition, in order to further study the influence of ion adsorption and triboelectric effect for the SL-TENG, the surface charge density changes of the DL-TENG and SL-TENG are researched by using their transferred charges when they are continuously operated. It can be seen that the surface charge density of the DL-TENG increases with the operation time of the TENG and then remains steady (Figure 3d). The reason behind this is that with the continuous operation of the TENG, the triboelectric effect accumulates the charge on the dielectric surface until the maximum surface charge density is reached and then the charge remains stable. Meanwhile, it is obvious that the surface charge density of the SL-TENG fabricated by PVC, PTFE, and FEP increases first and then decreases slowly, which is completely different from the surface charge density of

DL-TENG fabricated by the same dielectric material (Figure 3e). The corresponding reason is that the triboelectric effect of the SL-TENG is larger than the ion adsorption effect at the beginning, and then the ion adsorption effect gradually exceeds the triboelectric effect. In order to verify the above analysis, the surface charge density change of the SL-TENG fabricated by the electret FEP (E-FEP), which has a saturated surface charge, is also studied (Figure 3f). Because the sufficient surface charge is saturated, only the ion adsorption weakens the surface charge density at first and the triboelectric effect does not increase the surface charge density. It is obvious that the related surface charge decays directly, which well verifies the above analysis. Therefore, it is an important research direction of high-performance SL-TENGs to improve the triboelectric performance and weaken the ion adsorption effect of dielectric materials through material optimization.

2.4. Anticorrosion Performance of the SL-TENG.

Marine corrosion usually causes serious damage to the metal structure of various marine equipment including ships, thus affecting their function and safety. Figure 4a displays the mechanism of the most common marine corrosion of steel in seawater; it shows that the iron atoms on the steel surface as the anode lose their electrons to become ferrous iron (Fe^{2+}) and escape from the main body of steel into the seawater and then result in the irreversible structural damage of steel. Simultaneously, the water molecules and dissolved oxygen in seawater obtain the electrons lost at the anode as a cathode and reduce to produce hydroxide ions. Based on the above mechanism, providing more electrons in time to supplement the electrons lost by steel and reducing its own electrons to weaken its ability to lose electrons so as to maintain the

stability of the steel structure are two useful strategies to improve the marine anticorrosion of steel in the ocean. Many previous studies have focused on the former research by utilizing direct-current electricity from the TENG (Figure S17).^{30,31} However, the fabrication is extremely complicated due to the additional rectifier, the addition of the counter electrode, and the packaging of the TENG for wave-energy-collection TENGs. Besides, usage of simple simulated seawater by using a 3.5% sodium chloride (NaCl) solution is difficult to research real marine corrosion. Meanwhile, this method is extremely complex and difficult to integrate with the moving marine equipment such as ships to achieve the function of marine anticorrosion. According to the working principle of SL-TENGs, since the potential of uncoated steel electrodes can rise during the operative process of the SL-TENG, the ability of losing electrons on the uncoated steel electrode can be greatly weakened and endow the property of marine anticorrosion (Figure S18). In order to verify the relevant principles, we designed a test device consisting of a potentiostat, a Pt electrode as a reference electrode, and the SL-TENG fabricated by PTFE to monitor the potential change of the uncoated steel electrode in the SL-TENG (Figure 4b). Figure 4c shows the corresponding experimental result, and it is apparent that the potential of the steel electrode relative to the Pt electrode can basically stay at about -896 mV under the operation of the SL-TENG and gradually decreases to about -945 mV when the SL-TENG stops working. When the SL-TENG starts up again, the potential of the steel electrode relative to the platinum electrode rises rapidly again. Therefore, this result shows that the SL-TENG can weaken the ability of the steel electrode by losing electrons and achieve the marine anticorrosive property. In order to further verify the above principle, we have tested the potential of three kinds of copper, iron, and aluminum metal materials with different corrosion resistance values relative to the platinum electrode in seawater (Figure S19). Based on the known corrosion resistance sequence of the three metal materials and the corresponding experimental results, it can be found that the higher the potential of the relative platinum electrode, the more the corrosion resistance. Therefore, since the electric potential of the uncoated steel electrode relative to the platinum electrode can be increased during the operation of the SL-TENG, the SL-TENG can also improve the marine anticorrosion function of steel materials immersed in seawater. In addition, in order to better verify the marine anticorrosive function of the SL-TENG with the uncoated steel electrode, we record the microscopic images of the surface of the uncoated steel electrode in the SL-TENG and steel immersed in seawater alone at different times. The microscopic images of the uncoated steel electrode in the SL-TENG at different times are displayed in Figure 4d–e, and the microscopic images of steel immersed in seawater alone are depicted in Figure 4g–i (the magnification of the microscope is chosen to be 130 times), which indicates that compared with the corrosion of steel immersed in seawater alone, the uncoated steel electrodes in the SL-TENG remains more stable after 7 h and 18 h of immersion in seawater. As the simple structure of the SL-TENG can be easily integrated with the moving marine equipment such as ships, it provides an effective method for obtaining a metal marine anticorrosive for moving marine equipment.

3. CONCLUSIONS

In summary, a SL-TENG, which can be fabricated by a dielectric film as the organic coating and the coated and uncoated steel hull as the two electrodes, was prepared. The rational selection of the dielectric film enables the SL-TENG achieve an excellent output performance by the good triboelectrification performance and weak ion adsorption effect. Besides, compared with the CMACs, the friction coefficient of the SL-TENG with seawater is about half of that of the CMACs, which can assist in the building of ships to obtain a low sailing resistance of ships. More importantly, since the uncoated steel electrode that is even immersed in seawater has a high potential, it can yield a metal marine anticorrosive with good function. In a word, this work provides an effective method for designing metal marine anticorrosives for the development of marine science and technology.

4. EXPERIMENTAL SECTION

4.1. Fabrication of the TENGs. **4.1.1. Fabrication of the SS-TENG.** Different dielectric materials with PTFE, PVC, FEP (50 mm \times 100 mm), a copper foil (40 mm \times 60 mm), a foam (50 mm \times 100 mm), and an acrylic sheet (50 mm \times 100 mm \times 5 mm) were attached as a stator. The copper foil (30 mm \times 50 mm) and acrylic sheet (30 mm \times 50 mm) were attached as sliding electrodes.

4.1.2. Fabrication of the DL-TENG or SL-TENG. First, different dielectric materials with PTFE, PVC, FEP (125 mm \times 145 mm), a copper foil (120 mm \times 140 mm), and a double-sided adhesive tape with a polyimide material (125 mm \times 145 mm) were stuck together. Then, they were fixed on an acrylic tube with a diameter of 4.5 cm and a length of 15 cm. Besides, a copper foil or a Q235 carbon steel of dimensions 5 cm \times 7 cm was used as another counter electrode for the SL-TENG. Meanwhile, the relative DI water which has a conductivity of 18.4 M Ω -cm is generated by a pure water machine. Finally, the natural seawater used in this experiment comes from the coastal region Qingdao, PR China, which has a pH of about 8.0 and a salinity of 3.3%.

4.2. Electrical Measurement of the TENGs. The transferred charge, short-circuit current, and open-circuit voltage were monitored by a programmable electrometer (Keithley model 6514). The potential change of the steel electrode in the SL-TENG was recorded by a potentiostat (Biologic, VMP3). A linear motor (E1100) was used to obtain the patterns of movement with certain parameters for the SS-TENG, DL-TENG, and SL-TENG. An optical microscope with a magnification of 130 times was used to observe the surface morphology of steel.

■ ASSOCIATED CONTENT

Supporting Information

The Supporting Information is available free of charge at <https://pubs.acs.org/doi/10.1021/acsami.1c23575>.

Measuring principle of the frictional force of the water droplet on the material surface; theoretical analysis of seawater with ion adsorption on the dielectric surface and the test method of the SS-TENG with the open-circuit voltage; SEM image of the PTFE surface; schematic diagram of the electrical double layer; schematic diagram of the structural design of the SL-TENG; inclination angle of a water droplet that begins to slide on a different material; frictional force of a water droplet on a different material; photo of the seawater contact angle on a different material; SEM image of the PVC and FEP surface; photo of a seawater droplet on the inclined surface with different materials; comparison of the rolling torque of a seawater droplet on the inclined surface with different materials; schematic

diagram of the structural design of the DL-TENG; schematic diagram of ion adsorption on the dielectric surface; output performance of the SL-TENG and DL-TENG fabricated by nylon; output performance of the SS-TENG; schematic diagram of the structural design and working principle of the SS-TENG; circuit diagram of the SS-TENG with the voltage test; corresponding voltage of resistance by using the partial voltage method; principle of marine anticorrosion achieved by collecting the water wave energy as the power source through the TENG; principle of marine anticorrosion realized through the SL-TENG; and potential of three kinds of metal materials with different corrosion resistance values relative to the platinum electrode in seawater (PDF)

AUTHOR INFORMATION

Corresponding Author

Jie Wang – Beijing Institute of Nanoenergy and Nanosystems, Chinese Academy of Sciences, Beijing 100083, P. R. China; College of Nanoscience and Technology, University of Chinese Academy of Sciences, Beijing 100049, P. R. China; Center on Nanoenergy Research, School of Physical Science and Technology, Guangxi University, Nanning 530004, P. R. China; orcid.org/0000-0003-4470-6171; Email: wangjie@binn.cas.cn

Authors

Chuguo Zhang – Beijing Institute of Nanoenergy and Nanosystems, Chinese Academy of Sciences, Beijing 100083, P. R. China; College of Nanoscience and Technology, University of Chinese Academy of Sciences, Beijing 100049, P. R. China

Baofeng Zhang – Beijing Institute of Nanoenergy and Nanosystems, Chinese Academy of Sciences, Beijing 100083, P. R. China; College of Nanoscience and Technology, University of Chinese Academy of Sciences, Beijing 100049, P. R. China

Wei Yuan – Beijing Institute of Nanoenergy and Nanosystems, Chinese Academy of Sciences, Beijing 100083, P. R. China; College of Nanoscience and Technology, University of Chinese Academy of Sciences, Beijing 100049, P. R. China

Ou Yang – Beijing Institute of Nanoenergy and Nanosystems, Chinese Academy of Sciences, Beijing 100083, P. R. China; College of Nanoscience and Technology, University of Chinese Academy of Sciences, Beijing 100049, P. R. China

Yuebo Liu – Beijing Institute of Nanoenergy and Nanosystems, Chinese Academy of Sciences, Beijing 100083, P. R. China; Center on Nanoenergy Research, School of Physical Science and Technology, Guangxi University, Nanning 530004, P. R. China

Lixia He – Beijing Institute of Nanoenergy and Nanosystems, Chinese Academy of Sciences, Beijing 100083, P. R. China; College of Nanoscience and Technology, University of Chinese Academy of Sciences, Beijing 100049, P. R. China

Zhihao Zhao – Beijing Institute of Nanoenergy and Nanosystems, Chinese Academy of Sciences, Beijing 100083, P. R. China; College of Nanoscience and Technology, University of Chinese Academy of Sciences, Beijing 100049, P. R. China

Linglin Zhou – Beijing Institute of Nanoenergy and Nanosystems, Chinese Academy of Sciences, Beijing 100083, P. R. China; College of Nanoscience and Technology,

University of Chinese Academy of Sciences, Beijing 100049, P. R. China

Zhong Lin Wang – Beijing Institute of Nanoenergy and Nanosystems, Chinese Academy of Sciences, Beijing 100083, P. R. China; School of Materials Science and Engineering, Georgia Institute of Technology, Atlanta, Georgia 30332, United States; orcid.org/0000-0002-5530-0380

Complete contact information is available at:
<https://pubs.acs.org/10.1021/acsami.1c23575>

Author Contributions

C.Z., B.Z., and W.Y. contributed equally to this work. J.W. and Z.L.W. proposed and supervised the project. C.Z. participated in all aspects of this work from device fabrication to characterization and data processing. B.Z. and W.Y. assisted in the device fabrication and characterization. Y.L. participated in the drawing of schematic diagrams of related structures. O.Y. and L.H. assisted in the collection and processing of relevant data. Z.Z. and L.Z. provided a simple aid to the relevant experiment. All authors discussed the results and commented in the article.

Notes

The authors declare no competing financial interest.

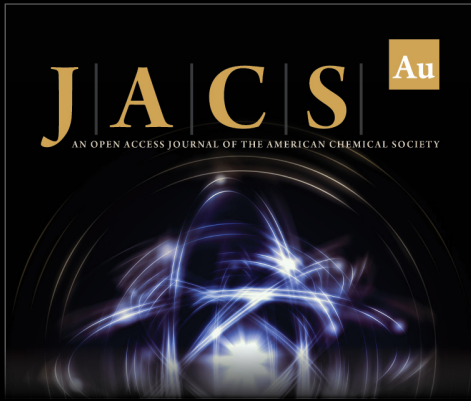
ACKNOWLEDGMENTS

This research was supported by the National Key R & D Project from the Ministry of Science and Technology (2016YFA0202704), National Natural Science Foundation of China (grant nos. 61774016, 21773009, and 22109013), Beijing Municipal Science and Technology Commission (Z171100000317001, Z171100002017017, and Y3993113DF), Key Research Program of Frontier Sciences, Chinese Academy of Sciences (ZDBS-LY-DQC025), and Fundamental Research Funds for the Central Universities (E1E46802). The authors also thank Haining Yu for the revision of this work in the progress of writing.

REFERENCES

- (1) Mollison, D.; Buneman, O. P.; Salter, S. H. Wave Power Availability in the Ne Atlantic. *Nature* **1976**, *263*, 223–226.
- (2) Zhang, C.; He, L.; Zhou, L.; Yang, O.; Yuan, W.; Wei, X.; Liu, Y.; Lu, L.; Wang, J.; Wang, Z. L. Active Resonance Triboelectric Nanogenerator for Harvesting Omnidirectional Water-Wave Energy. *Joule* **2021**, *5*, 1613–1623.
- (3) Wang, Z. L. Catch wave power in floating nets. *Nature* **2017**, *542*, 159–160.
- (4) Zhang, B.; Zhu, Q.; Li, Y.; Hou, B. Facile Fluorine-Free One Step Fabrication of Superhydrophobic Aluminum Surface towards Self-cleaning and Marine Anticorrosion. *Chem. Eng. J.* **2018**, *352*, 625–633.
- (5) Zhang, L.; Shan, C.; Jiang, X.; Li, X.; Yu, L. High Hydrophilic Antifouling Membrane Modified with Capsaicin-Mimic Moieties via Microwave Assistance (MWA) for Efficient Water Purification. *Chem. Eng. J.* **2018**, *338*, 688–699.
- (6) Zhong, Y.; Guo, Y.; Wei, X.; Rui, P.; Du, H.; Wang, P. Multi-Cylinder-Based Hybridized Electromagnetic-Triboelectric Nanogenerator Harvesting Multiple Fluid Energy for Self-Powered Pipeline Leakage Monitoring and Anticorrosion Protection. *Nano Energy* **2021**, *89*, 106467.
- (7) Chen, R.; Zhang, Y.; Xie, Q.; Chen, Z.; Ma, C.; Zhang, G. Transparent Polymer-Ceramic Hybrid Antifouling Coating with Superior Mechanical Properties. *Adv. Funct. Mater.* **2021**, *31*, 2011145.

- (8) Wang, Z.; Cheng, L.; Zheng, Y.; Qin, Y.; Wang, Z. L. Enhancing the Performance of Triboelectric Nanogenerator through Prior-Charge Injection and Its Application on Self-powered Anticorrosion. *Nano Energy* **2014**, *10*, 37–43.
- (9) Zhang, Y.; Huo, Z.; Wang, X.; Han, X.; Wu, W.; Wan, B.; Wang, H.; Zhai, J.; Tao, J.; Pan, C.; Wang, Z. L. High Precision Epidermal Radio Frequency Antenna via Nanofiber Network for Wireless Stretchable Multifunction Electronics. *Nat. Commun.* **2020**, *11*, 5629.
- (10) Zhang, C.; Liu, L.; Zhou, L.; Yin, X.; Wei, X.; Hu, Y.; Liu, Y.; Chen, S.; Wang, J.; Wang, Z. L. Self-Powered Sensor for Quantifying Ocean Surface Water Waves Based on Triboelectric Nanogenerator. *ACS Nano* **2020**, *14*, 7092–7100.
- (11) Li, X.; Yin, X.; Wang, W.; Zhao, H.; Liu, D.; Zhou, L.; Zhang, C.; Wang, J. Carbon Captured from Vehicle Exhaust by Triboelectric Particulate Filter as Materials for Energy Storage. *Nano Energy* **2019**, *56*, 792–798.
- (12) Guo, H.; Pu, X.; Chen, J.; Meng, Y.; Yeh, M. H.; Liu, G.; Tang, Q.; Chen, B.; Liu, D.; Qi, S.; Wu, C.; Hu, C.; Wang, J.; Wang, Z. L. A Highly Sensitive, Self-Powered Triboelectric Auditory Sensor for Social Robotics and Hearing Aids. *Sci. Rob.* **2018**, *3*, No. eaat2516.
- (13) Zhang, C.; Zhou, L.; Cheng, P.; Liu, D.; Zhang, C.; Li, X.; Li, S.; Wang, J.; Wang, Z. L. Bifilar-Pendulum-Assisted Multilayer-Structured Triboelectric Nanogenerators for Wave Energy Harvesting. *Adv. Energy Mater.* **2021**, *11*, 2003616.
- (14) Zhang, C.; Liu, Y.; Zhang, B.; Yang, O.; Yuan, W.; He, L.; Wei, X.; Wang, J.; Wang, Z. L. Harvesting Wind Energy by a Triboelectric Nanogenerator for an Intelligent High-Speed Train System. *ACS Energy Lett.* **2021**, *6*, 1490–1499.
- (15) Chen, L.; Chen, C.; Jin, L.; Guo, H.; Wang, A. C.; Ning, F.; Xu, Q.; Du, Z.; Wang, F.; Wang, Z. L. Stretchable Negative Poisson's Ratio Yarn for Triboelectric Nanogenerator for Environmental Energy Harvesting and Self-Powered Sensor. *Energy Environ. Sci.* **2021**, *14*, 955–964.
- (16) Wang, H.; Xu, L.; Bai, Y.; Wang, Z. L. Pumping up the Charge Density of a Triboelectric Nanogenerator by Charge-Shuttling. *Nat. Commun.* **2020**, *11*, 4203.
- (17) Leung, S.-F.; Fu, H.-C.; Zhang, M.; Hassan, A. H.; Jiang, T.; Salama, K. N.; Wang, Z. L.; He, J.-H. Blue Energy Fuels: Converting Ocean Wave Energy to Carbon-Based Liquid Fuels via CO₂ Reduction. *Energy Environ. Sci.* **2020**, *13*, 1300–1308.
- (18) Xu, W.; Zheng, H.; Liu, Y.; Zhou, X.; Zhang, C.; Song, Y.; Deng, X.; Leung, M.; Yang, Z.; Xu, R. X.; Wang, Z. L.; Zeng, X. C.; Wang, Z. A Droplet-Based Electricity Generator with High Instantaneous Power Density. *Nature* **2020**, *578*, 392–396.
- (19) Zhang, B.; Wu, Z.; Lin, Z.; Guo, H.; Chun, F.; Yang, W.; Wang, Z. L. All-in-one 3D Acceleration Sensor Based on Coded Liquid-Metal Triboelectric Nanogenerator for Vehicle Restraint System. *Mater. Today* **2021**, *43*, 37.
- (20) Wei, X.; Zhao, Z.; Zhang, C.; Yuan, W.; Wu, Z.; Wang, J.; Wang, Z. L. All-Weather Droplet-Based Triboelectric Nanogenerator for Wave Energy Harvesting. *ACS Nano* **2021**, *15*, 13200–13208.
- (21) Gu, H.; Zhang, N.; Zhou, Z.; Ye, S.; Wang, W.; Xu, W.; Zheng, H.; Song, Y.; Jiao, J.; Wang, Z.; Zhou, X. A Bulk Effect Liquid-Solid Generator with 3D Electrodes for Wave Energy Harvesting. *Nano Energy* **2021**, *87*, 106218.
- (22) Zhang, Q.; Jiang, C.; Li, X.; Dai, S.; Ying, Y.; Ping, J. Highly Efficient Raindrop Energy-Based Triboelectric Nanogenerator for Self-Powered Intelligent Greenhouse. *ACS Nano* **2021**, *15*, 12314–12323.
- (23) Tang, W.; Chen, B. D.; Wang, Z. L. Recent Progress in Power Generation from Water/Liquid Droplet Interaction with Solid Surfaces. *Adv. Funct. Mater.* **2019**, *29*, 1901069.
- (24) Lin, S.; Chen, X.; Wang, Z. L. Contact Electrification at the Liquid-Solid Interface. *Chem. Rev.* **2021**, 1c00176.
- (25) Cui, P.; Wang, J.; Xiong, J.; Li, S.; Zhang, W.; Liu, X.; Gu, G.; Guo, J.; Zhang, B.; Cheng, G.; Du, Z. Meter-Scale Fabrication of Water-Driven Triboelectric Nanogenerator Based on in-situ Grown Layered Double Hydroxides through a Bottom-up Approach. *Nano Energy* **2020**, *71*, 104646.
- (26) Liu, X.; Cui, P.; Wang, J.; Shang, W.; Zhang, S.; Guo, J.; Gu, G.; Zhang, B.; Cheng, G.; Du, Z. A Robust All-Inorganic Hybrid Energy Harvester for Synergistic Energy Collection from Sunlight and Raindrops. *Nanotechnology* **2021**, *32*, 075401.
- (27) Shang, W.; Gu, G.; Zhang, W.; Luo, H.; Wang, T.; Zhang, B.; Guo, J.; Cui, P.; Yang, F.; Cheng, G.; Du, Z. Rotational Pulsed Triboelectric Nanogenerators Integrated with Synchronously Triggered Mechanical Switches for High Efficiency Self-Powered Systems. *Nano Energy* **2021**, *82*, 105725.
- (28) Zhu, H. R.; Tang, W.; Gao, C. Z.; Han, Y.; Li, T.; Cao, X.; Wang, Z. L. Self-Powered Metal Surface Anti-Corrosion Protection Using Energy Harvested from Rain Drops and Wind. *Nano Energy* **2015**, *14*, 193–200.
- (29) Cui, S.; Zheng, Y.; Liang, J.; Wang, D. Conducting Polymer PPy Nanowire-Based Triboelectric Nanogenerator and Its Application for Self-Powered Electrochemical Cathodic Protection. *Chem. Sci.* **2016**, *7*, 6477–6483.
- (30) Pang, H.; Feng, Y.; An, J.; Chen, P.; Han, J.; Jiang, T.; Wang, Z. L. Segmented Swing-Structured Fur-Based Triboelectric Nanogenerator For Harvesting Blue Energy toward Marine Environmental Applications. *Adv. Funct. Mater.* **2021**, *31*, 2106398.
- (31) Sun, W.; Zheng, Y.; Li, T.; Feng, M.; Cui, S.; Liu, Y.; Chen, S.; Wang, D. Liquid-Solid Triboelectric Nanogenerators Array and Its Applications for Wave Energy Harvesting and Self-Powered Cathodic Protection. *Energy* **2021**, *217*, 119388.
- (32) Nie, J.; Ren, Z.; Xu, L.; Lin, S.; Zhan, F.; Chen, X.; Wang, Z. L. Probing Contact-Electrification-Induced Electron and Ion Transfers at a Liquid-Solid Interface. *Adv. Mater.* **2019**, *32*, 1905696.
- (33) Xu, M.; Wang, S.; Zhang, S. L.; Ding, W.; Kien, P. T.; Wang, C.; Li, Z.; Pan, X.; Wang, Z. L. A Highly-Sensitive Wave Sensor Based on Liquid-Solid Interfacing Triboelectric Nanogenerator for Smart Marine Equipment. *Nano Energy* **2019**, *57*, 574–580.



JACS Au
AN OPEN ACCESS JOURNAL OF THE AMERICAN CHEMICAL SOCIETY

Editor-in-Chief
Prof. Christopher W. Jones
Georgia Institute of Technology, USA

Open for Submissions 

pubs.acs.org/jacsau  ACS Publications
Most Trusted. Most Cited. Most Read.